Stochastic Dynamic Trapping in Robotic Manipulation of Micro-objects Using Optical Tweezers

Xiao Yan, Chien Chern Cheah, Quang Minh Ta, and Quang-Cuong Pham

***Abstract*—Various automatic manipulation techniques have been developed for manipulating micro-objects using optical tweezers. Because of the small trapping force of optical traps and of increase in kinetic energy during manipulation, a trapped object may not remain trappable especially in the presence of random Brownian perturbation. However, there is no theoretical analysis so far to help understand the effects of the dynamic motion and Brownian forces on the trappability problem of optical tweezers. This paper investigates the optical manipulation of micro-objects under random perturbations. Here we provide for the first time a theoretical and experimental analysis of dynamic trapping problem from stochastic perspectives. We derive the relationship between trapping probability and maximum manipulation velocity. A controller with appropriate velocity bound is then proposed to ensure that the system is bounded and stable. The experimental results confirm the accuracy of our theoretical analysis and illustrate the necessity and usefulness of the proposed controller.**

***Index Terms*—Optical tweezers, micromanipulation, dynamic trapping, Brownian motion, stochastic control.**

I. Introduction

The rapid developments in robotic technology and microfabrication process have drawn significant attention to robotic-aided biomedical applications over the last decades. Some of the representative applications include microinjection [1]–[3], microgripper [4], [5], and microrobot [6]–[10]. Compared with traditional manual manipulations with tools such as micropipettes, systems integrated with robotic technology and biomedical equipments make micromanipulations easier yet with more accuracy, precision, and efficiency.

Various techniques have been developed for the purpose of biomedical-related manipulations of micro-objects, such as magnetic tweezers [11], dielectrophoresis (DEP) [12], [13], and atomic force microscopy (AFM) [14], [15], among others. These techniques impose however various restrictions including the type of micro-objects that can be manipulated and the environment in which the micro-objects should be manipulated [16]. Take magnetic tweezers for example, a magnetic bead is usually attached to the object of interest such that the object can be manipulated in the time-varying magnetic field. Biological cells manipulated by DEP will experience voltages during the manipulation process which may cause damages to the cells. For AFM, a potential risk is that the AFM tips may collide with the object surfaces and thus cause damages. Furthermore, it is difficult in AFM to acquire real-time images of the manipulation process.

X. Yan, C. C. Cheah, and Q. M. Ta are with the School of Electrical and Electronic Engineering, Nanyang Technological University, Singapore.

Q. -C. Pham is with the School of Mechanical and Aerospace Engineering, Nanyang Technological University, Singapore.

This work was supported by the Agency for Science, Technology and Research of Singapore under Grant 1121202014.

With a tightly focused laser beam, optical tweezers [17]–[19] can generate forces to attract micro-objects with various sizes around the vicinity of the beam focus [20]. A freely diffusing micro-object can thus be trapped and manipulated by changing the position of the beam focus. This simple but effective non-contact manipulation approach with high precision has therefore been extensively utilized in such applications as cell transportation [21], cell sorting [22], [23], cell-cell interactions [24], and cell migration [25]. Traps arrays can be generated and manipulated using holographic optical tweezers system with the help of spatial light modulators [26], [27]. Four dimensional optical manipulation was reported and interactive particle position control can be achieved forming arbitrary volumetric constellations and complex three-dimensional trajectories in real time [28].

Robotic-aided optical tweezers have been further investigated and applied in biomedical applications with automatic control approaches. In [29], a three-axis steering system was developed for optical tweezers and the trapped micro-object serves as a measurement probe. Automated cell transportation was reported in [30] with calibrated optimal motion parameters and a modified path planning algorithm. Automated trapping, assembly and sorting of colloidal objects was reported at the microscale with closed loop holographic optical tweezers [31]. A stochastic dynamic programming framework was proposed for automated particle transport operations in [32]. A novel control and planning approach was presented for automated and indirect manipulation of cells using silica beads arranged into gripper formations, employing path planning and feedback control for efficient collision-free transport of a cell between two specified locations [33]. An integrated closed-loop controller was developed in [34], allowing the transition from trapping to manipulation without any hard switching from one controller to another. Vision based observer technique was presented in [35] to estimate the velocity of cell without the need of camera calibration. In [36], dynamic interaction between the cell and the manipulator of laser source was studied and a setpoint control approach was proposed, which was further extended to a region reaching controller. Automated manipulation of multiple non-spherical objects was proposed in [37] by using multiple-force optical clamps. An automated arraying approach was developed in [38] to place groups of micro-objects into a predefined array with right pairs using holographic optical tweezers. Patterning of a group of cells was considered in [39] with a multilevel-based topology design, which can form various desired patterns with rotation and scaling capabilities. To minimize the exposure of the cell to the laser beam, an indirect pushing based automated micromanipulation of biological cells was reported in [40]. Dynamic coordination of multiple groups of cells was investigated to

achieve time-varying multi-cellular formation [41]. Optical tweezers could also be integrated with other technologies such as microfluidic devices [42], exhibiting great potential and flexibility for further developments and applications. In [43], Brownian motion was considered and the authors proposed an estimation and optimal control schemes to decrease the effect of the random perturbations – without being able to cancel it completely. Considering the Brownian effect on nanoparticles, a feedback control approach was introduced to increase the trapping lifetime of nanoparticles by more than an order of magnitude without increasing laser power [44].

The trapping force of the optical trap is very small and there is also a gain in kinetic energy by the trapped object during manipulation. Therefore, the object that is static trappable while not in motion may not remain trappable during manipulation, especially in the presence of random Brownian perturbation. However, there is no theoretical analysis so far to help understand the effects of the dynamic motion and Brownian forces on the trappability problem of optical tweezers. Here, we investigate the effects of random perturbations on the trappability of micro-objects. Although Brownian motion has been known for a long time, the random Brownian term is not often modelled in the dynamics of optical manipulations. The system without considering Brownian motion is not an accurate modelling the dynamics of small micro-objects since Brownian motion significantly affects the behavior of small micro-objects. Therefore, random Brownian motion must be modelled and included in the system dynamics. For those works which took account for the Brownian motion, the models were usually solved by simulations. A radial basis function based approach was proposed to generate simplified models for estimating the trapping probability in optical trapping experiments using offline simulations [45].

In this paper, the dynamics of the trapped object is analyzed using tools from stochastic calculus [46], [47]. Specifically, in Section III, we determined the relationship between the probability that the micro-object remains trapped during a time interval and the maximum manipulation velocity. We used this for two different approaches: one based on stochastic Lyapunov theory [46] and one based on a direct analysis of the object motion – which can be associated with an Ornstein–Uhlenbeck process [48], [49]. The proposed method provides a theoretical foundation for understanding the dynamic trapping problem. The theoretical values of maximum manipulation velocity and trapping probability can be calculated instantly offline without the help of simulations. The effects of parameters including trapping stiffness, size of micro-objects and manipulation time on the maximum manipulation velocity and trapping probability are also explicitly shown to gain insights into the dynamic trapping problem. In Section IV, a controller with appropriately chosen manipulation velocity is then proposed and analyzed. Finally, in Section V experimental results are presented to illustrate the accuracy of our theoretical analysis, as well as the necessity and usefulness of the proposed controller.

A preliminary version of this paper was accepted for presentation in [50]. This paper presents an extended version which includes a new analysis based on Ornstein–Uhlenbeck process. The new approach is compared with the Lyapunov method presented in [50] and shown to be more accurate. New experimental results using different sizes of trapped objects are also presented.

II. Theory and model description

In this section, the Brownian motion is defined as a stochastic process. The dynamics of a freely diffusing micro-object in fluid is presented, and earlier results on static optical trapping are briefly reviewed.

A. Brownian motion

Definition 1: A standard Brownian motion (one-dimensional) is a stochastic process $\{W_t : t \geq 0\}$ with the following properties [51]

1) W_t is continuous in the parameter t, and $W_0 = 0$;
2) for every $0 \leq t_1 < t_2 < t_3 < \cdots < t_n$, the increments $W_{t_2} - W_{t_1}$, $W_{t_3} - W_{t_2}$, $\cdots$, $W_{t_n} - W_{t_{n-1}}$) are independent random variables;
3) for each $0 \leq s < t < +\infty$, the increment $W_t - W_s$ is a Gaussian random variable with mean 0 and variance $t - s$.

We shall also use the notation $\xi = \frac{dW_t}{dt}$. The process ξ is called Gaussian white noise and satisfies

$$\langle \xi(t) \rangle = 0, \tag{1}$$

$$\langle \xi(t)\xi(t') \rangle = \delta(t - t'). \tag{2}$$

where $t' \geq 0$, Dirac's function $\delta(t)$ is equal to zero for all $t \neq 0$. For $t = 0$, $\delta(t) = 1$.

□

Assuming there exists no external potential, the Brownian object is considered as "free", and the motion of the "free" Brownian object in two dimensional space is modeled by the Langevin equation [52]

$$\boldsymbol{M}\ddot{\boldsymbol{x}} = -\boldsymbol{\Gamma}\dot{\boldsymbol{x}} + \boldsymbol{F}, \tag{3}$$

where $\boldsymbol{x} = [x_1, x_2]^T$ is the object position, $\boldsymbol{M} = \mathrm{diag}(m, m)$ with object mass m, $\boldsymbol{\Gamma} = \mathrm{diag}(\gamma_1, \gamma_2)$ is the drag coefficient, $\boldsymbol{F} = \sqrt{2k_B\mathcal{T}}[\sqrt{\gamma_1}\xi_1, \sqrt{\gamma_2}\xi_2]^T$ denotes the two-dimensional Brownian force, k_B is the Boltzmann constant, $\mathcal{T}$ is the absolute temperature, ξ_1 and ξ_2 are two independent realizations of ξ (we shall drop the subscript when there is no ambiguity).

For manipulation of micro-objects, the Reynolds number is always low ($Re \ll 1$) for the environment, and thus the inertia effect in (3) could be ignored and yields

$$\boldsymbol{\Gamma}\dot{\boldsymbol{x}} = \boldsymbol{F}. \tag{4}$$

The inertia term will be ignored in the rest of the paper.

B. Static optical trapping

Static trapping of a micro-object refers to the situation when the laser is static with respect to the solution, as shown in Fig. 1. The potential energy U of the gradient force is determined by many factors, including intensity and wavelength of the incident light, object size, and the refractive indices of the object and the medium. The conditions for

a stable static trapping in a single beam trap are discussed in [17], and one necessary and sufficient condition is that the potential well of the gradient force should be much larger than the kinetic energy of the Brownian objects, which is described by $\exp(-U/k_B\mathcal{T}) \gg 1$. This requirement can be seen as requiring the time to pull the object into an optical trap much less than the time for the object to diffuse out of the trap because of Brownian motion [17]. Therefore the minimum energy for a stable static trapping in a single beam trap could be calculated constraining $|U|_{min} > 10k_B\mathcal{T}$ [17].

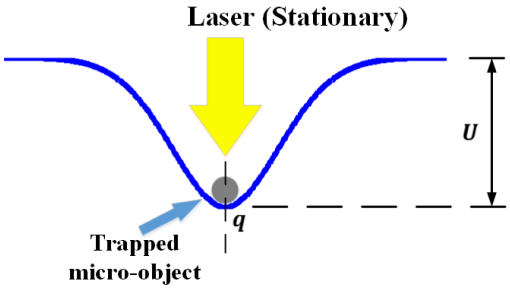

Fig. 1. Static trapping of a micro-object: the micro-object is trapped by a laser beam with fixed position. The distance between the center of laser beam and center of micro-object is zero for static trapping.

III. Dynamic trapping and maximum manipulation velocity

When the optical trap is moving together with the laser, the trapped object gains additional kinetic energy due to the motion, making it easier to escape from the optical trap, which is considered as a *dynamic optical trapping* problem. The trapped object should be manipulated within a certain threshold velocity, otherwise it may escape from the optical trap if manipulated at a high velocity. The following sections are devoted to the derivation of this threshold velocity.

A. Cell dynamics and dynamic trapping probability

Consider a moving trapped micro-object as shown in Fig. 2, whose cell dynamics in each dimension can be described as

$$\dot{x}_i = \frac{k(x,q)}{\gamma_i}(q_i - x_i) + \sqrt{2D_i}\xi \tag{5}$$

where $\boldsymbol{q} = [q_1, q_2]^T$ is the laser position, $D_i = \frac{k_B\mathcal{T}}{\gamma_i}$ is the diffusion constant, and $k(x,q)$ is the optical trapping stiffness defined as [34], [53]

$$k(x,q) = \begin{cases} k_c, & |q_i - x_i| \le R_i \\ k_c e^{-k_R(|q_i-x_i|-R_i)^2}, & |q_i - x_i| > R_i \end{cases}, \tag{6}$$

where k_c and k_R are positive constants, and R_i is the trapping distance in each dimension satisfying $R_1^2 + R_2^2 = R^2$ where R is the overall trapping radius. An illustration of the trapping stiffness and trapping force are shown in Fig. 3(a) and Fig. 3(b), respectively.

Definition 2: A micro-object is dynamically trapped for a total manipulation time T if there exists a laser trajectory $\boldsymbol{q}(t)$ such that $\|\boldsymbol{q}(t) - \boldsymbol{x}(t)\| \le R$ for $t \in [0,T]$. The

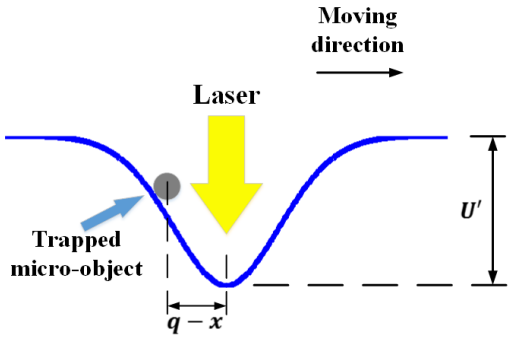

Fig. 2. Dynamic trapping of a micro-object: the micro-object is trapped by a laser beam and manipulated with certain speed. The distance between the center of laser beam and center of micro-object is $|q-x|$ for dynamic trapping.

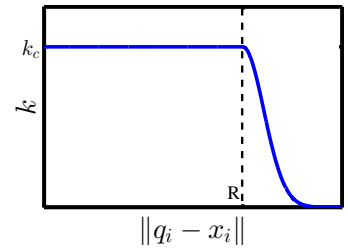

(a) trapping stiffness

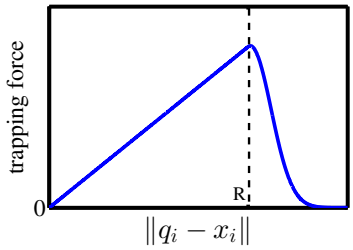

(b) trapping force

Fig. 3. Trapping stiffness and trapping force. The trapping stiffness is defined to be constant within the trapping radius.

dynamic trapping probability describes the possibility of the object remains trapped for a total manipulation time T such that $\|\boldsymbol{q}(t) - \boldsymbol{x}(t)\| \le R$ when the laser is in motion. □

A sufficient condition to ensure $\|\boldsymbol{q}(t) - \boldsymbol{x}(t)\| \le R$ is that $|q_i - x_i| \le R_i = \frac{\sqrt{2}}{2}R$ for $i = 1, 2$. Therefore, by defining $R_1 = R_2 = \frac{\sqrt{2}}{2}R$, we have the following sufficient condition for dynamic trapping.

Definition 3: The sufficient condition for dynamic trapping in each dimension for a total manipulation time T is the probability $P\left(\forall t \le T, |q_i - x_i| \le \frac{\sqrt{2}}{2}R\right)$ in each dimension. The overall dynamic trapping probability in two dimensional space for a total manipulation time T can be determined as

$$P\left(\forall t \le T, \sum_{i=1}^{2}(q_i - x_i)^2 \le R^2\right) \ge \prod_{i=1}^{2} P\left(\forall t \le T, |q_i - x_i| \le R_i = \frac{1}{\sqrt{2}}R\right). \tag{7}$$

□

When $|q_i - x_i| \leq R_i$, the cell dynamics in each dimension can then be expressed as

$$\dot{x}_i = \rho_i(q_i - x_i) + \sqrt{2D_i}\xi, \tag{8}$$

where $\rho_i = \frac{k_c}{\gamma_i}$ with maximum trapping stiffness k_c.

As illustrated in Fig. 4, a object is trapped and in motion. Although the trapped object is still within the optical trap, it does not necessarily guarantee the trapping of the object at all time due to several possible reasons, including the random Brownian motion, and the gained kinetic energy as the trapped object is in motion, which may lead to the escape of the object from the optical trap. To understand the effect of manipulation velocity v_i for $i = 1, 2$ and the Brownian motion on the dynamic optical trapping problem, we assume the laser moves with a positive constant velocity v_i such that its position is given by $q_i = v_i t + \frac{v_i}{\rho_i} + x_{i0}$, where x_{i0} is the initial position of the object, and the velocity satisfying $v_i \leq \rho_i R_i$.

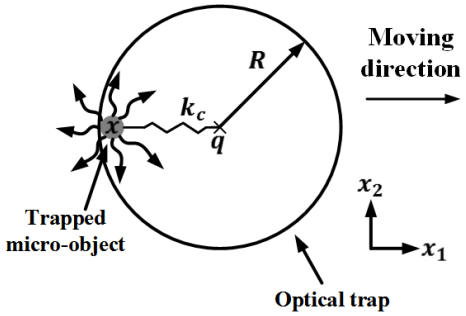

Fig. 4. Random behavior of a trapped object due to Brownian motion: the trapped micro-object may move in any direction due to Brownian motion when at the verge of the optical trap, and may escape from the moving laser trap.

Define a new variable $y_i = (\rho_i/D_i)^{1/2}(x_i - q_i + \frac{v_i}{\rho_i})$ and express equation (8) in terms of y_i as

$$\dot{y}_i = -\rho_i y_i + \sqrt{2\rho_i}\xi, \tag{9}$$

where y_i is an Ornstein–Uhlenbeck (O–U) process [54]. The above equation can be written in the form of Itô stochastic differential equation as

$$dy_i = -\rho_i y_i dt + \sqrt{2\rho_i} dW_t. \tag{10}$$

Note that the position of y_i at $t = 0$ is now zero.

Since $x_i - q_i = (D_i/\rho_i)^{1/2} y_i - \frac{v_i}{\rho_i}$, the dynamic trapping probability in each dimension becomes $P\left(\forall t \leq T, |(D_i/\rho_i)^{1/2} y_i - \frac{v_i}{\rho_i}| \leq R_i\right)$. Therefore, the overall two-dimensional dynamic trapping probability with a constant velocity v_i over a total manipulation time T can be determined as

$$\begin{aligned} &P\left(\forall t \leq T, \|\boldsymbol{q} - \boldsymbol{x}\| \leq R\right) \\ &= \prod_{i=1}^{2} P\left(\forall t \leq T, |(D_i/\rho_i)^{1/2} y_i - \frac{v_i}{\rho_i}| \leq R_i\right). \end{aligned} \tag{11}$$

It can be easily concluded that $|(D_i/\rho_i)^{1/2} y_i - \frac{v_i}{\rho_i}| \leq R_i$ is guaranteed if $|(D_i/\rho_i)^{1/2} y_i| \leq R_i - \frac{v_i}{\rho_i}$. The dynamic trapping probability in each dimension is defined as

$$P\left(\forall t \leq T, |(D_i/\rho_i)^{1/2} y_i| \leq R_i - \frac{v_i}{\rho_i}\right). \tag{12}$$

Therefore, the overall two-dimensional dynamic trapping probability can be obtained as

$$\begin{aligned} &P\left(\forall t \leq T, \|\boldsymbol{q} - \boldsymbol{x}\| \leq R\right) \\ &\geq \prod_{i=1}^{2} P\left(\forall t \leq T, |y_i| \leq (\rho_i/D_i)^{1/2}(R_i - \frac{v_i}{\rho_i})\right) \end{aligned} \tag{13}$$

In the next sections, we will present the following two results: (1) dynamic trapping probability in each dimension when the trapped object is manipulated with constant velocity v_i for a total manipulation time T; (2) maximum manipulation velocity $v_i^{\max}$ in each dimension given a desired dynamic trapping probability P_i^{des} for a total manipulation time T.

B. Sufficient conditions for dynamic trapping based on stochastic Lyapunov analysis

Lyapunov method has been utilized extensively for stability analysis in deterministic systems, and it can also be applied to the analysis of stochastic system [46], [47]. In this section, Lyapunov method is used to derive a relationship between the trapping probability and the maximum manipulation velocity.

We define the Lyapunov function candidate

$$V_i(t) = y_i^2, \tag{14}$$

whose derivative is

$$\begin{aligned} \mathscr{L}V_i(t) &= \frac{\partial V}{\partial t} + \frac{\partial V}{\partial y_i}(-\rho_i y_i) + \frac{1}{2} tr(2\sqrt{2\rho_i} I_1) \\ &= -2\rho_i y_i^2 + 2\rho_i = -2\rho_i V_i(t) + 2\rho_i, \end{aligned} \tag{15}$$

where $\mathscr{L}$ denotes the differential generator of the Itô process [46].

Let $c_i^2 = (\rho_i/D_i)(R_i - \frac{v_i}{\rho_i})^2$. Using results on *finite time stability* (cf. chapter III in [46]), one obtains the following lower bound on the dynamic trapping probability in each dimension for a total manipulation time T

$$\begin{aligned} P\left(\forall t \leq T, y_i^2 < c_i^2\right) &= 1 - P\left(\forall t \leq T, \sup y_i^2 \geq c_i^2\right) \\ &\geq \left(1 - \frac{y_i^2(0)}{c_i^2}\right) e^{-\Phi/c_i^2} \\ &= \exp\left(-\Phi_i/c_i^2\right) \\ &= \exp\left(-\frac{2D_i T}{(R_i - \frac{v_i}{\rho_i})^2}\right), \end{aligned} \tag{16}$$

where $y_i(0) = 0$, and $\Phi_i = 2\rho_i T$.

Therefore, for a given constant laser velocity v_i over a total manipulation time T, the a lower bound for the dynamic trapping probability in each dimension can be obtained as

$$P\left(\forall t \leq T, |y_i| \leq (\rho_i/D_i)^{1/2}(R_i - \frac{v_i}{\rho_i})\right) \geq \exp\left(-\frac{2D_i T}{(R_i - \frac{v_i}{\rho_i})^2}\right). \tag{17}$$

On the other hand, for a given one dimensional desired trapping probability P_i^{des} over a total manipulation time T, the maximum manipulation velocity $v_i^{\max}$ is constrained as

$$v_i^{\max} = \rho_i \left(R_i - \sqrt{\frac{2D_i T}{|\ln P_i^{\text{des}}|}} \right) = \frac{k_c}{\gamma_i} \left(R_i - \sqrt{\frac{2k_B \mathcal{T} T}{\gamma_i |\ln P_i^{\text{des}}|}} \right). \tag{18}$$

This value of $v_i^{\max}$ can be negative, in which case it is considered as 0.

Note that the above results are based on a *lower bound* of the trapping probability and can therefore be overly conservative. In particular, $v_i^{\max}$ decreases as the negative square-root of the total manipulation time T. Fig. 5 shows for instance that, for a desired trapping probability of 0.95, $v_i^{\max}$ reaches 0 for $T \geq 5s$. In practice, however, the total manipulation time affects the maximum manipulation velocity only weakly. This observation prompted us to develop a finer approach.

C. Sufficient conditions for dynamic trapping based on direct analysis of the Ornstein–Uhlenbeck process

Here, we study directly equation (10) in order to obtain tighter bounds for the trapping probability, and subsequently, the maximum manipulation velocity.

Consider the change of variable $\tau = \rho_i t$. We have $dW_\tau = \sqrt{\rho_i} dW_t$. Substituting τ into (10) yields

$$dy_i = -y_i d\tau + \sqrt{2} dW_\tau \tag{19}$$

which is the normalized O–U process [48], [49]. Consider a bound $c_i > 0$ and assume that $y_i(0) = 0$. The probability for the random variable y_i to remain in $(-c_i, c_i)$ for all time instants $\tau \in (0, T^*)$ is given by [49]

$$P(\forall \tau \leq T^*, |y_i| < c_i) \simeq e^{-\lambda(-c_i, c_i) T^*}, \tag{20}$$

where $\lambda(-c_i, c_i)$ is the smallest positive zero of $M(-\lambda/2, 1/2, c_i^2/2)$, where M is the confluent hypergeometric function of the first kind [48].

Note that, for the approximation (20) to be valid, c_i must be sufficiently large, verifying

$$\int_{c_i}^{\infty} e^{-y_i^2/2} \ll 1. \tag{21}$$

It has be shown that this criterion is verified for $c_i \geq 3$. In this case, the actual probability is essentially indistinguishable from the asymptotics [49].

Next, for sufficiently large c_i, $\lambda(-c_i, c_i)$ can be approximated by [48]

$$\lambda(-c_i, c_i) \simeq \frac{c_i}{\exp(c_i^2/2)} \sqrt{\frac{2}{\pi}}. \tag{22}$$

The approximation error for $\lambda(-c_i, c_i)$ is around 10% for $c_i = 3$, and drops within 5% for $c_i \geq 5$ [48], [49]. Therefore, the approximation (22) can be used when $c_i \geq 5$.

We thus have

$$P(\forall \tau_i \leq T^*, |y_i| < c_i) \simeq \exp\left(-T^* \sqrt{\frac{2}{\pi}} \cdot \frac{c_i}{\exp(c_i^2/2)} \right). \tag{23}$$

As a result, given a total manipulation time T and a manipulation velocity v_i, we have

$$P\left(\forall t \leq T, |y_i| < c_i\right) \simeq \exp\left(-\rho_i T \sqrt{\frac{2}{\pi}} \cdot \frac{c_i}{\exp(c_i^2/2)} \right), \tag{24}$$

where

$$c_i = \sqrt{\rho_i / D_i} \left(R_i - \frac{v_i}{\rho_i} \right) \tag{25}$$

Conversely, given a total manipulation time T and a desired trapping probability P_i^{des} (for example $P_i^{\text{des}} = 0.95$), the barrier c_i^{des} can be found by solving

$$\frac{c_i^{\text{des}}}{\exp({c_i^{\text{des}}}^2/2)} = -\frac{\ln(P_i^{\text{des}})}{\rho_i T} \sqrt{\frac{\pi}{2}}. \tag{26}$$

Next, the maximum manipulation velocity is given by

$$v_i^{\max} = \frac{k_c}{\gamma_i} \left(R_i - c_i^{\text{des}} \sqrt{\frac{k_B \mathcal{T}}{k_c}} \right) \tag{27}$$

Note that a negative result of $v_i^{\max}$ suggests the object can not be trapped dynamically. We can now state the following proposition.

Proposition 1: Consider a micro-object that is manipulated by a laser beam in two-dimensional space with a constant velocity v_i in each dimension. The probability that the object remains trapped in each dimension for a total manipulation time T is given by equation (24) and (25). The two-dimensional dynamic trapping probability is given by $P_{2\text{D}} = P_1 P_2$.

Conversely, given a desired dynamic trapping probability P_i^{des} in each dimension, the maximum velocity in each dimension is given by equations (26) and (27).

□

D. Discussion

Here, we compare the dynamic trapping probability and maximum manipulation velocity obtained by the Lyapunov approach and the direct approach. We also discuss the parameters affecting the results.

We consider a $5\mu m$ latex microbead in deionized water (viscosity $10^{-3}\,\text{Pa}\cdot\text{s}$), laser power 0.1W, overall trapping radius $R = 5.1\mu m$, trapping stiffness $k_{ci} = 1.3pN/\mu m$, temperature $\mathcal{T} = 300K$.

For manipulation velocity $v_i = 40\mu m/s$, Fig. 5 shows the dynamic trapping probabilities as a function of the manipulation time T. The probability given by the Lyapunov analysis decreases very quickly towards zero. On the contrary, the probability obtained by the direct analysis depends only weakly on time, which is consistent with experiments.

Assume now that the desired trapping probability is given as $P_i^{\text{des}} = 0.95$, and let us compute the maximum manipulation velocity such that the object remains trapped for all times $t \in (0, T)$ with probability P_i^{des}. Fig. 6 shows $v^{\max}$ as a function of T for two different trapping stiffness. As mentioned previously, the Lyapunov analysis yielded too conservative bounds, which decrease very quickly to 0.

Next, remark that, for trapping stiffness $k_{ci} = 1.3pN/\mu m$ (Fig. 6a), the $v^{\max}$ computed by the direct analysis is very

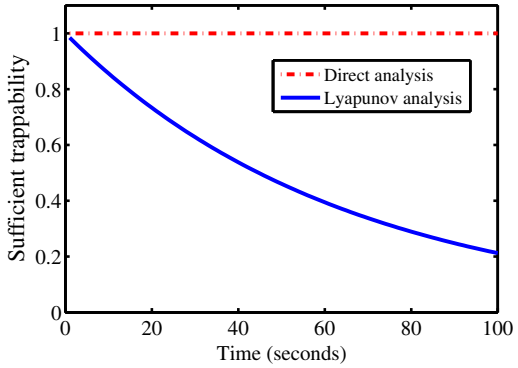

Fig. 5. Comparison of dynamic trapping probabilities given by the Lyapunov approach and the direct approach. Both methods are time dependent and time is a crucial factor for the Lyapunov approach but not for the direct approach.

close (about 90%) to the that without considering Brownian motion ($v_i = \rho_i R_i$), indicating that the Brownian effect is not significant at this level of laser power. However, for a weaker trapping stiffness $k_{ci} = 1.3 \times 10^{-2} pN/\mu m$ (Fig. 6b), the result obtained by direct analysis drops to about 40% of the value without considering Brownian motion for $T = 100$ s, indicating the significance of the Brownian effect for low laser powers.

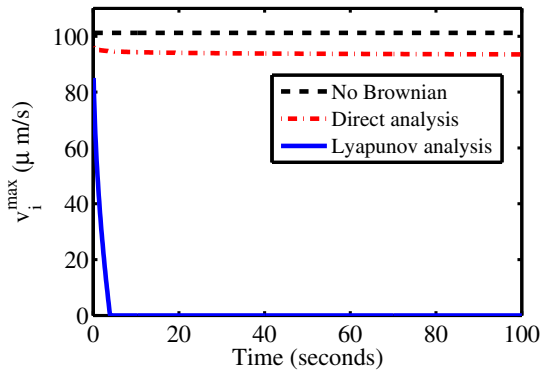

(a) $k_{ci} = 1.3 pN/\mu m$

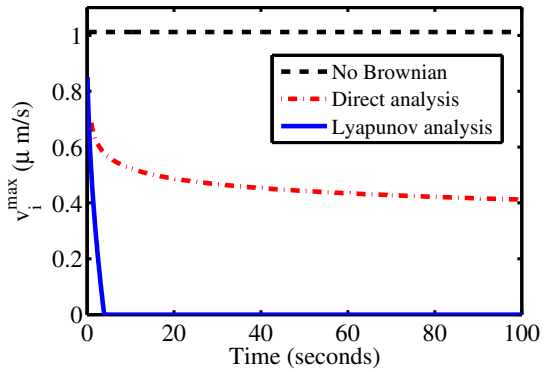

(b) $k_{ci} = 1.3 \times 10^{-2} pN/\mu m$

Fig. 6. Comparison of $v_i^{\max}$ between two approaches. The results show the effects of time and trapping stiffness on the maximum manipulation speeds. When laser power is small, the Brownian motion could not be ignored since it would greatly affect the maximum manipulation speed.

From equations (17), (18), (24), and (27), it appears that the dynamic trapping probability and the maximum manipulation velocity are dependent on several parameters, including laser power (trapping stiffness), viscosity, object radius, absolute temperature, and manipulation time. The following table presents the results of qualitative analysis on the effects of these different parameters on the dynamic trapping probability and maximum manipulation velocity, where the symbol "?" indicates that there is no definite conclusion in this case.

	Trapping probability		v_{max}	
	Lyapunov	OU	Lyapunov	OU
T_{temp} ↑	↓	↓	↓	↓
T ↑	↓	↓	↓	↓
R ↑	↑	↑	↑	↑
Power ↑	↑	↑	↑	↑
Viscosity ↑	?	?	↓	↓

TABLE I
EFFECTS OF DIFFERENT PARAMETERS ON TRAPPING PROBABILITY AND MAXIMUM MANIPULATION SPEED

Note that the effect of object radius is not shown in the table since the object radius is coupled with other parameters including the maximum trapping stiffness [55] and the results are thus complicated. Take the maximum manipulation velocity for example, we analyze $v_i^{\max}$ from several regimes. Consider the Rayleigh regime ($r \ll \lambda_{\text{laser}}$) where r is the object radius and λ_{laser} is the wavelength of the laser beam, the overall trapping radius R is constant [55], and k_c varies as r^3 [56]. The increase in r results in the increase in $v_i^{\max}$ for both approaches. For Ray optics regime ($r \gg \lambda_{\text{laser}}$), the overall trapping radius R is linear with the object radius r, and k_c will decrease as the trapping force will be independent of r in this regime. Considering the magnitude of change, further increase of r will lead to lower $v_i^{\max}$. Although conclusions can be made in these two regimes, the intermediate regime ($r \sim \lambda_{\text{laser}}$) is still complicated as the change in k_c is unclear in this intermediate regime (between r^0 and r^3, [56]).

Based on Fig. 6, the $v_i^{\max}$ from the direct analysis is compared with the maximum velocity without considering Brownian motion ($v_i = \rho_i R_i$). We consider the ratio between $c_i^{\text{des}} \sqrt{\frac{k_B \mathcal{T}}{k_c}}$ and R_i in equation (27), and the larger ratio indicates the more significant effect in velocity constraint due to Brownian motion. Increasing manipulation time and temperature, or decreasing laser power or object radius, can all contribute to a larger ratio, which is consistent with understanding of Brownian effect and experimental observations. Note that the change in time and absolute temperature will only cause tiny change in c_i^{des} and $\mathcal{T}$. However, when the object radius r and laser power are small ($c_i^{\text{des}} \sqrt{\frac{k_B \mathcal{T}}{k_c}}$ and R_i are of the same scale), the random Brownian effect to the object will become significant (consistent with Fig. 6), which should not be ignored during real applications.

IV. Manipulation controller design with dynamic trapping

Most existing optical manipulation approaches ignored the random effect of Brownian motion, and control methods were developed assuming that the trapped object will never escape. Saturated controllers can be implemented to alleviate this problem but there is no theoretical result to analyze the stability of the optical manipulation system in the presence of Brownian motion. In this section, a saturated controller with appropriately chosen manipulation velocity is presented to keep the micro-object trapped for a given time during manipulation and the stability analysis of the system is presented based on Lyapunov-like stochastic approach.

Consider a trapped micro-object in two dimensions with fixed vertical position. Similar to the one dimensional case, the dynamics of the trapped object is described as:

$$\boldsymbol{\Gamma}\dot{\boldsymbol{x}} = k(\boldsymbol{x},\boldsymbol{q})(\boldsymbol{q}-\boldsymbol{x}) + \boldsymbol{F}, \tag{28}$$

where $k(\boldsymbol{x},\boldsymbol{q}) = \mathrm{diag}(k(x,q), k(x,q))$.

Definition 4: Given positive constant M, a function $s: R \to R : \zeta \mapsto s(\zeta)$ is defined as a saturation function with bound M, if it is non-decreasing, and satisfies the following properties:

1) $\zeta s(\zeta) > 0, \forall \zeta \neq 0$;
2) $|s(\zeta)| \leq M, \forall \zeta \in R$.

□

A saturation vector is defined as $\mathbf{sat}() = [s_1(), s_2()]^T$ where $s_i(), i = 1,2$ are strictly increasing and continuously differentiable saturation functions defined as:

$$s_i(z) = \begin{cases} a(M_i-1) + a\tanh(z/a - (M_i-1))], \\ \qquad \text{if } z > a(M_i-1) \\ z, \\ \qquad \text{if } a(M_i-1) \leq z \leq a(M_i-1) \\ -a(M_i-1) + a\tanh(z/a + (M_i-1)))], \\ \qquad \text{if } z < -a(M_i-1) \end{cases} \tag{29}$$

where a is a positive scaling factor, and $M_i > 1$ is a constant.

An illustration of the saturation function $s_i()$ is shown in Fig. 7. It can be seen that the saturation function $s_i()$ is an odd function, and is linear within the non-saturation zone, i.e. $[-a(M_i-1), a(M_i-1)]$. It can be seen that $|s_i()| \leq aM_i$, where $aM_i = v_i^{\max}, i = 1,2$ in both directions.

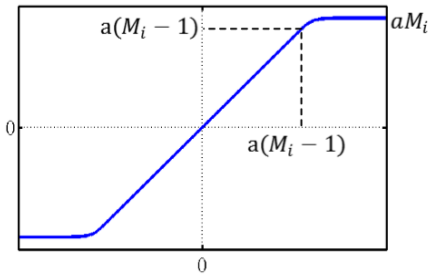

Fig. 7. Saturation function is defined to be strictly increasing and continuously differentiable.

The desired velocity of the micro-object $\dot{\boldsymbol{x}}_d$ is designed to be within the non-saturation zone $[-a(M_i-1), a(M_i-1)]$ in both dimensions, satisfying the follows:

$$\sup \|\dot{\boldsymbol{x}}_d\| < \|\boldsymbol{v}^{\max}\| = \sqrt{|v_1^{\max}|^2 + |v_2^{\max}|^2} \tag{30}$$

where $\boldsymbol{x}_d(t)$ is the desired trajectory of the object. This is reasonable as given a maximum manipulation velocity obtained from Eqn. (27), the desired velocity of the object should not be planned in such a way that it exceeds the maximum manipulation velocity.

However, $\dot{\boldsymbol{x}}_d$ is bounded does not necessarily indicate the boundedness of $\dot{\boldsymbol{x}}$. Consider the transient phase, i.e. when the initial position of the micro-object $\boldsymbol{x}_0$ is far from the initial position of the desired trajectory. The large initial position error might result in a high initial velocity which could cause the trapped object to escape at the beginning of the manipulation, even though the desired velocity satisfies equation (30). Therefore, a controller should be appropriately developed to ensure the boundedness of $\dot{\boldsymbol{x}}$.

The position input for the laser beam is proposed based on the saturation vector functions as:

$$\boldsymbol{q} = \boldsymbol{x} - k^{-1}(\boldsymbol{x},\boldsymbol{q})\boldsymbol{\Gamma} \cdot \mathbf{sat}(K_p\Delta\boldsymbol{x} - \dot{\boldsymbol{x}}_d). \tag{31}$$

where $\Delta\boldsymbol{x} = \boldsymbol{x} - \boldsymbol{x}_d$.

Substituting (31) into (28) yields:

$$\dot{\boldsymbol{x}} = -\mathbf{sat}(K_p\Delta\boldsymbol{x} - \dot{\boldsymbol{x}}_d) + \boldsymbol{D}\boldsymbol{\Xi}, \tag{32}$$

where $\boldsymbol{D} = \mathrm{diag}(\sqrt{2D_1}, \sqrt{2D_2})$, $D_i = \frac{k_B\mathcal{T}}{\gamma_i}$ for $i = 1,2$, and $\boldsymbol{\Xi} = [\xi_1, \xi_2]^T$. It can be seen that the velocity of the object $\dot{\boldsymbol{x}}$ has been constrained. The term $K_p\Delta\boldsymbol{x} - \dot{\boldsymbol{x}}_d$ is constrained in this case since constraining $\Delta\boldsymbol{x}$ will produce more conservative bounds.

Since the desired velocity $\dot{\boldsymbol{x}}_d$ satisfies the constraint as in (30), $\dot{\boldsymbol{x}}_d$ can be written as $\mathbf{sat}(\dot{\boldsymbol{x}}_d)$. Subtracting both sides of equation (32) by $\dot{\boldsymbol{x}}_d$, we have:

$$\Delta\dot{\boldsymbol{x}} = \dot{\boldsymbol{x}} - \dot{\boldsymbol{x}}_d = -\mathbf{sat}(K_p\Delta\boldsymbol{x} - \dot{\boldsymbol{x}}_d) - \mathbf{sat}(\dot{\boldsymbol{x}}_d) + \boldsymbol{D}\boldsymbol{\Xi}, \tag{33}$$

which can be written in the form of stochastic differential equation:

$$d(\Delta\boldsymbol{x}) = -(\mathbf{sat}(K_p\Delta\boldsymbol{x} - \dot{\boldsymbol{x}}_d) + \mathbf{sat}(\dot{\boldsymbol{x}}_d))dt + \boldsymbol{D}d\boldsymbol{W}. \tag{34}$$

where $\boldsymbol{W} = [W_1, W_2]^T$ denotes the two-dimensional Brownian motion with distinct and independent W_1 and W_2.

We define a Lyapunov-like function candidate as:

$$V(t) = \frac{1}{2}\Delta\boldsymbol{x}^T\Delta\boldsymbol{x}. \tag{35}$$

Theorem: Consider a system described by (28) with control input given in (31), then $\forall t \geq 0$

$$E[V(t)] \leq \frac{D_1+D_2}{\lambda_1} + \left[V(0) - \frac{D_1+D_2}{\lambda_1}\right]^+ e^{-2\lambda_1 t} \tag{36}$$

where $[.]^+ = \max(0,.)$ and $E[V(t)]$ is the conditional expectation of $V(t)$ given that the object stays trapped (note that all the expectations below are conditional to the same event, whose probability is calculated in Section III).

Proof: We derive an inequality on $\mathscr{L}V(t)$ where $\mathscr{L}$ denotes the differential generator of the Itô process (see Appendix).

$$\begin{aligned}\mathscr{L}V(t) &= -\frac{\partial V}{\partial \Delta \boldsymbol{x}}(\mathbf{sat}(K_p\Delta \boldsymbol{x} - \dot{\boldsymbol{x}}_d) + \mathbf{sat}(\dot{\boldsymbol{x}}_d)) \\ &\quad + \frac{1}{2}tr((2D_1 + 2D_2)I_2) \\ &= -\Delta \boldsymbol{x}^T(\mathbf{sat}(K_p\Delta \boldsymbol{x} - \dot{\boldsymbol{x}}_d) \\ &\quad + \mathbf{sat}(\dot{\boldsymbol{x}}_d)) + 2(D_1 + D_2). \end{aligned} \tag{37}$$

Consider one dimension of the first term in (37). Since saturation function **sat**() is an odd function and the gain K_p is positive, we can see $s_1(K_p\Delta x_1 - \dot{x}_{1d}) + s_1(\dot{x}_{1d}) = s_1(K_p\Delta x_1 + (-\dot{x}_{1d})) - s_1(-\dot{x}_{1d})$. Since $s_1()$ is a strictly increasing odd function, the sign of $s_1(K_p\Delta x_1 - \dot{x}_{1d}) + s_1(\dot{x}_{1d})$ is the same as the sign of Δx_1, which is represented by $k_1\Delta x_1$ with positive gain k_1. Therefore, the first term in (37) can be written in the form of $-(k_1\Delta x_1^2 + k_2\Delta x_2^2)$ with positive k_1 and k_2. Thus, we have $\mathscr{L}V(t) \leq -\lambda_1\|\Delta \boldsymbol{x}\|^2 + 2(D_1 + D_2)$, where $\lambda_1 = \min(k_1, k_2)$. Next,

$$\mathscr{L}V(t) \leq -2\lambda_1 V(t) + 2(D_1 + D_2), \tag{38}$$

which yields, by Dynkin's formula [46]

$$E[V(t)] - V(0) = E\left[\int_0^t \mathscr{L}V(s)ds\right]. \tag{39}$$

Therefore $\forall u, t,\ 0 \leq u \leq t < +\infty$

$$\begin{aligned} &E[V(t)] - E[V(u)] = E\left[\int_u^t \mathscr{L}V(s)ds\right] \\ &\leq E\left[\int_u^t (-2\lambda_1 V(s) + 2(D_1 + D_2))ds\right] \\ &= \int_u^t (-2\lambda_1 E[V(s)] + 2(D_1 + D_2))ds. \end{aligned} \tag{40}$$

Based on the Gronwall-type lemma [47], we have $\forall t \geq 0$

$$E[V(t)] \leq \frac{D_1 + D_2}{\lambda_1} + \left[V(0) - \frac{D_1 + D_2}{\lambda_1}\right]^+ e^{-2\lambda_1 t}, \tag{41}$$

which means that the mean square error between the object trajectory and the desired trajectory is bounded, and the system described by (28) and (31) is stable.

□

Remark 1. The proposed controller is model based with the assumption that the model is exactly known but there is a certain degree of robustness to model uncertainty [57]. However, the tracking error may increase with uncertain parameters and thus adaptive control must be employed to deal with the increasing tracking error [57].

V. Experiments

Experiments were performed to demonstrate the effectiveness of the proposed approaches for manipulations of micro-objects. Without lost of generosity, the maximum manipulation velocity is considered to be positive, and hence the maximum manipulation velocity is referred as maximum manipulation speed for experimental results in this section.

A. Experimental setup and methods

An optical manipulation system (Elliot Scientific) mounted on an anti-vibration table (Thorlabs) was used in our experiments as shown in Fig. 8. Main sensors of this system include a microscope (Nikon Eclipse T*i*) and a CCD camera (Basler AG) with a resolution of 640x480 and frame rate of 30 fps. An oil immersion objective lens of 100x magnification was used to observe the microenvironment. The size of each pixel under 100x was 0.074 μm, and the size of the field of view is 47.36 μm in length and 35.52 μm in width. A motorized stage (Marzhauser Wetzlar) can be controlled manually with a joystick or automatically by the computer to achieve desired movements. A highly focused laser beam (Ytterbium Fibre Laser, IPG Photonics) can be generated with the near-infrared wavelength of 1070 nm. Multiple traps can be generated as well to manipulate multiple micro-objects concurrently. The Image Processing VI of Labview is directly applied for real time location of the micro-objects given certain parameters, including threshold value, target size, and etc. Labview is used for various purposes, including programming, image processing, localization of cell positions, and data recording, etc.

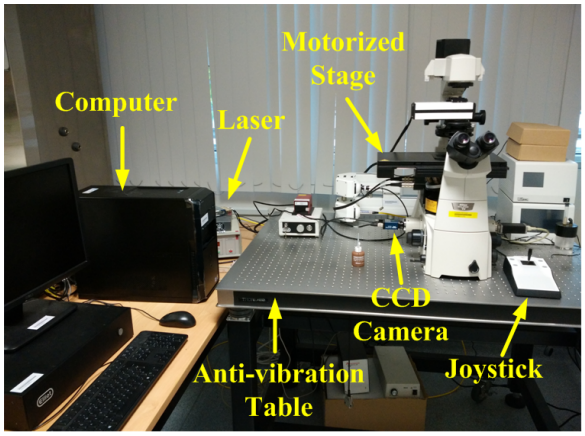

Fig. 8. Experimental setup

There are two approaches to estimate experimentally the maximum manipulation speed: (a) fix the position of the motorized stage and move the laser trap; (b) fix the position of the laser trap and move the motorized stage. By experimental observations, we found these two methods lead to different results, and the maximum speed obtained by method (a) was smaller than (b). The reason for this could be explained as follows. While the laser trap was moving, the laser beam might be slightly bent as shown in Fig. 9(a), which may lead to a decrease of the trapping force along the direction of the drag force, and consequently smaller maximum speed. When moving stage instead of the laser trap as shown in Fig. 9(b), the laser beam is always perpendicular to the stage, and thus the obtained maximum velocity was larger and more accurate. Therefore, the position of the laser trap was fixed and the motorized stage was manipulated in the experiments. The speed of the stage was increased step by step until the micro-object went off. If for a given speed, the object escaped

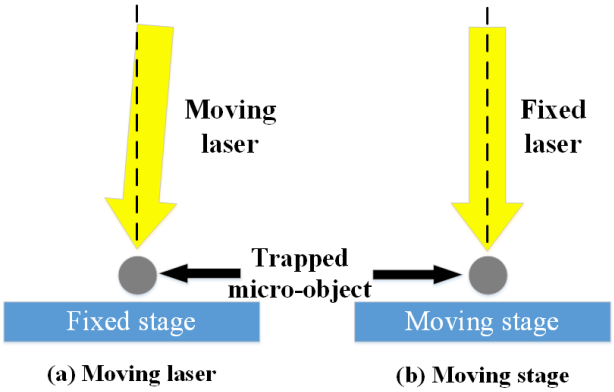

Fig. 9. Two different methods of measuring the maximum velocity: (a) fix the position of the motorized stage and move the laser trap; (b) fix the position of the laser trap and move the motorized stage. The laser beam might be slightly bent when moving the laser, which may lead to a decrease of the trapping force along the direction of the drag force, and consequently smaller maximum speed. In the experiment, the results were obtained by moving the motorized stage.

before $T = 5s$ then the previous speed was recorded as the value of the maximum manipulation velocity. This procedure was repeated 50 times per experimental condition. The average and standard deviation were computed over these 50 trials. Note that, all the experiments were performed only on the target micro-objects who were initially trapped stably with zero speed, i.e., stationary.

B. Results

Spherical latex microbeads with three different diameters (1 μm, 3 μm, 5 μm, Life Technologies, Singapore) were used in the experiments. Deionized water was used as the medium fluid. The laser power was set as 0.1 W, and only one microbead was trapped and manipulated each time. The trapping stiffness and trapping radius were measured and estimated with averaged values for the above mentioned objects by using the commercially purchased optical tweezers system from Elliot Scientific together with the image processing technique, and the results were listed in Table. II. The detailed information of trapping stiffness measurement can be found in [58].

1 μm bead	Trapping stiffness (pN/μm)	3.6
	Trapping radius (μm)	1.04
3 μm bead	Trapping stiffness (pN/μm)	1.9
	Trapping radius (μm)	3.04
5 μm bead	Trapping stiffness (pN/μm)	1.3
	Trapping radius (μm)	5.19

TABLE II
TRAPPING STIFFNESS AND TRAPPING RADIUS

Fig. 10 shows the experimental (average and standard deviation) maximum manipulation speed for 1 μm beads, the theoretical maximum manipulation speed if random perturbations are not taken into account, and the curve "trapping probability versus manipulation velocity" predicted by equations (26) and (27) (with $T = 5$ s). One can see if one does not take into account random perturbations, the computed maximum speed is significantly higher than the experimentally observed one, resulting in object loss during manipulation. On the other hand, the sharp transition in trapping probability (from 1 to 0) occurs at manipulation velocities very close to the experimental maximum speed. Thus, using the maximum speed corresponding to e.g. $P_i^{\text{des}} = 0.95$, one would in practice have a close estimate of the actual speed above which the object starts to escape. Fig. 11 and 12, show that these observations also hold for 3 μm, and 5 μm beads.

The comparison of the three tested bead sizes furthermore shows that the stochastic analysis is more and more indispensable (in the sense that the bound given by the deterministic analysis is less and less accurate) as the bead sizes become smaller.

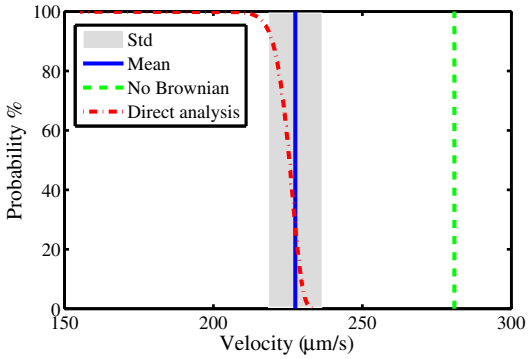

Fig. 10. Comparisons between theoretical and experimental results for 1 μm beads. The blue solid line is the average experimental maximum manipulation speed and the grey area represents the standard deviation. The red dashed curve shows the theoretical maximum manipulation speed obtained by direct analysis corresponding to various trapping probabilities. The theoretical value without considering Brownian motion is much higher than the direct analysis and the experimental results, indicating that the Brownian motion must be considered for micro-object with small sizes.

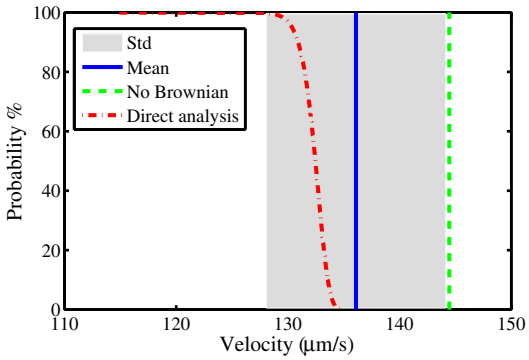

Fig. 11. Comparisons between theoretical and experimental results for 3 μm beads. The theoretical value without considering Brownian motion is close to the direct analysis and the experimental results, but still higher than the average experimental speed.

On the other hand, we experimentally obtained the success rate of manipulation given a desired probability. The theoretical speed bounds were determined by the direct analysis

Power: 0.1W	P_i^{des}=0.999			P_i^{des}=0.95		
	Direct analysis	Manipulation speed	Success rate	Direct analysis	Manipulation speed	Success rate
1 μm bead	155.3 μm/s	155 μm/s	100%	217.7 μm/s	217 μm/s	100%
3 μm bead	114.6 μm/s	114 μm/s	100%	130.4 μm/s	130 μm/s	100%
5 μm bead	86.6 μm/s	86 μm/s	100%	94.6 μm/s	94 μm/s	96%

TABLE III
SUCCESS RATE WITH DIFFERENT DESIRED PROBABILITIES

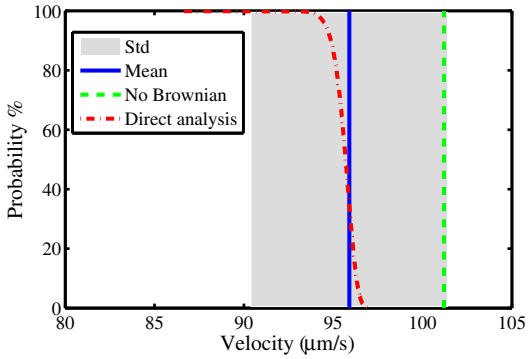

Fig. 12. Comparisons between theoretical and experimental results for 5 μm beads. The theoretical value without considering Brownian motion is close to the direct analysis and the experimental results, but still higher than the average experimental speed.

with $T = 5s$ for each object in 1D. Although the experiments were performed in 2D, the conservative value of maximum velocity for 1D case was chosen as the manipulation speed for each object since some parameters (trapping stiffness, trapping radius) may not be consistent at all places in the microenvironment. Two desired probabilities were presented and the final success rate were presented in Table. III. In all, it could be seen clearly that the proposed direct analysis provided a good estimation of the relationship between the manipulation speed and the dynamic trappability.

In the next experiment, to show the performance of the control approach, a 5 μm microbead was trapped and moved to converge to a fixed point. Only the microbead marked by "5 μm microbead" was trapped by laser, and the other microbeads were used as references to show the movement of the motorized stage since the background could not provide much information of the change of position. The position of the laser trap remained fixed and the motorized stage was manipulated. The control parameter K_p was set as $K_p = 20$. The initial position of trapped object with respect to the motorized stage was considered as the origin (0,0), and the desired object position with respect to the stage was set as (20 μm, 15 μm). The loop rate for the controller was 30Hz.

In the first case, the initial position of the object was shown in Fig. 13(a), and the controller was used without the speed bound, and resulted in the escape of the initially trapped microbead after only 0.15 second. In the second case, the speed bound for the proposed controller was set to 85 μm/s in each direction for dynamic trapping with 99.9% success rate. As shown in Fig. 14, the microbead was dynamically trapped at all time and finally reached at the desired position after 0.6 seconds. Note there was a large offset between the laser position and object center when the cell was manipulated with high speed as shown in Fig. 14(b)-(c). These results indicated the necessity of an appropriate speed bound even if the desired speed is set as zero in setpoint control. The positional errors were shown in Fig. 15, illustrating the performance of the proposed saturated control approach.

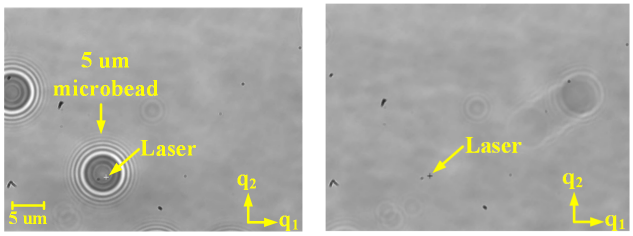

(a) t=0 (b) t=0.15s

Fig. 13. First case: fixed point control for the trapped 5 μm microbead without speed bound: (a) only the object marked as "5 μm microbead" was initially trapped by a laser trap (laser center "+" with the initially trapped microbead), and the position of the laser trap was fixed; (b) the motorized stage was manipulated without speed bound, and the initially trapped microbead escaped from the laser trap within 0.15s during the movement of the motorized stage (laser center "+" without the initially trapped microbead).

As the maximum speeds were different for various micro-objects, the approaches could be further used for optical filtering of objects without using image processing technique, even among different objects with similar sizes and shapes. Yeast cells with diameters around 5 μm were mixed with microbeads with 5 μm diameter, and the overall trapping stiffness and the trapping radius for the yeast cells were measured with the average of 0.9 pN/μm and 4.15 μm, respectively. The maximum speed within 5 seconds with 0.1% probability was determined as 53.5 μm/s by the direct analysis (i.e. 99.9% of the yeast cells would escape at this speed). With a manipulation speed set slightly higher as 60 m/s, the dynamic trapping probability for the yeast cell is nearly 0% while the dynamic trapping probability for the 5 μm bead is almost 100%. Since the maximum speeds were different for the yeast cells and 5 μm microbeads, it was thus applicable to filter them apart by a certain manipulation speed. The four mixed objects were initially trapped as shown in Fig. 16(a) and the total laser power was set to 0.4W such that the power for each trap was 0.1W. The initial position of the motorized stage was considered as the origin (0,0), and the desired position of the stage was set as (20 μm, 15 μm). The maximum manipulation speed was set to 60 μm/s in each direction for

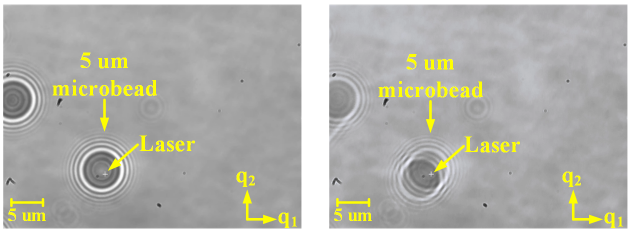

(a) t=0 (b) t=0.1s

(c) t=0.3s (d) t=0.6s

Fig. 14. Second case: fixed point control for the trapped 5 μm microbead with speed bound:(a) only the object marked as "5 μm microbead" was initially trapped by a laser trap (laser center "+" with the initially trapped microbead), and the position of the laser trap was fixed; (b)-(d) the motorized stage was manipulated with certain speed bound, and the microbead stayed trapped at all time and was manipulated to the desired position after 0.6s.

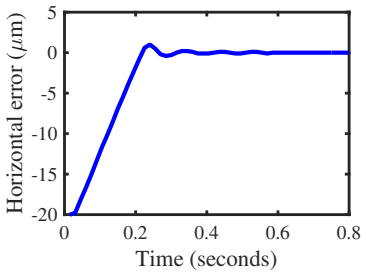

(a) Horizontal error

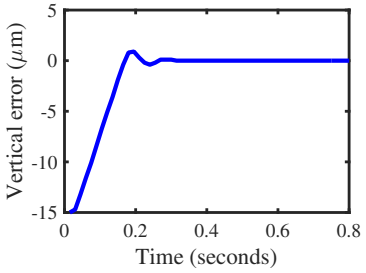

(b) Vertical error

Fig. 15. Positional errors for the trapped 5 μm microbead

the motorized stage. It could be seen from Fig. 16(b)-(f) that the yeast cells escaped from the traps approximately after 0.15 second, whereas the 5 μm microbeads stayed trapped at all time. Therefore, this approach could be one simple yet effective way to filter multiple mixed objects without using image processing techniques.

C. Discussions

Note that the dynamic trapping probability and the maximum manipulation velocity may subject to the dimension of

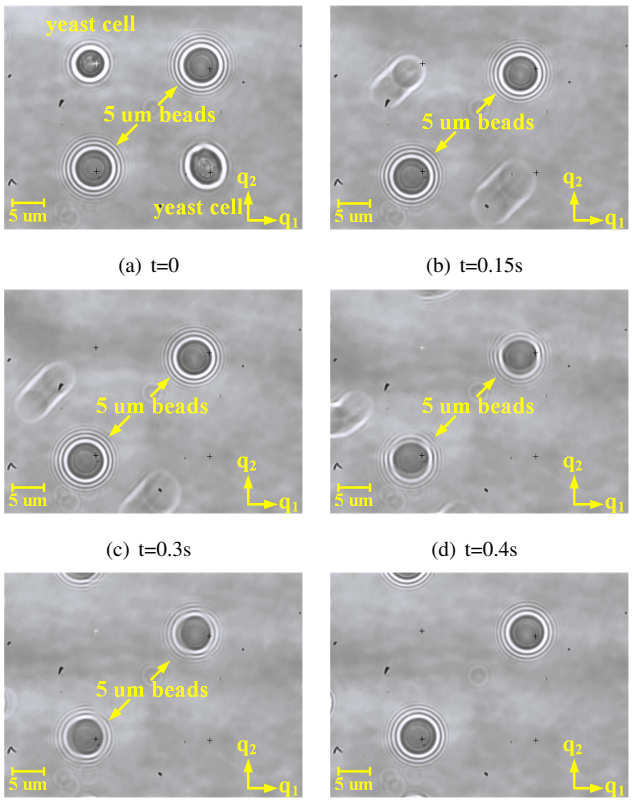

(a) t=0 (b) t=0.15s

(c) t=0.3s (d) t=0.4s

(e) t=0.5s (f) t=0.7s

Fig. 16. Optical filtering for different micro-objects. All the micro-objects were trapped by four fixed laser traps, and the motorized stage started to move with the speed of 60 μm/s. The 5 μm microbeads and the yeast cells were filtered apart within a tiny period.

the trajectory, i.e., 1D trajectory or 2D trajectory. Assuming that the trapping stiffness is identical in the horizontal and vertical directions, and if the maximum manipulation velocity is v_{max} with dynamic trapping probability of P for 1D case, then the maximum manipulation velocity for 2D case becomes $\sqrt{2}v_{max}$ with dynamic trapping probability of P^2. Therefore, in order to guarantee the manipulation velocity of v_{max} for 2D case with dynamic trapping probability of P, then the maximum velocity for 1D case is thus $v_{max}/\sqrt{2}$ with dynamic trapping probability of $\sqrt{P}$. Of course, these conditions are sufficient conditions.

For most experimental setups, it is not easy to accurately measure the trapping stiffness and the trapping radius. Usually, a set of data can be obtained for each parameter and the averaged values can be used if the standard deviations of the data sets are low. If the standard deviations are high, it is suggested to use the data that will lead to more conservative estimation of the manipulation velocities and trapping probabilities.

Based on our observations, the experimental results can be further improved in the future from several aspects. As the frame rate of the CCD camera is 30 fps, the time between two consecutive images is around 33 ms. When manipulated at high speed, say 150 μm/s, a trapped object can move around 5 μm within 33 ms, a distance that can not be ignored. Therefore, a high speed camera is necessary to improve the control outcome. Camera of high resolution will also help

in image processing, which gives better position and size estimation of the trapped micro-object. As the calibration of the optical tweezers is done from the beginning, the trap center on each trapped object may vary, leading to uncertain offset between the micro-object and trap center. Other challenges include the real temperature of the trapped micro-object as the laser will heat it up, and the limited magnification of the objective lens.

VI. Conclusions

In this paper, we have investigated the dynamic optical trapping of micro-objects under random perturbations. The relationship between trapping probability and maximum manipulation velocity has been derived based on two distinct methods. We have then designed a controller that takes into account this maximum manipulation velocity. Experimental results illustrated the performance of our theoretical analysis as well as the necessity and usefulness of the proposed controller. Taken together, the results presented in this paper provide guidelines for robotic-aided optical manipulation of micro-objects, a regime where random Brownian perturbations can lead to manipulation failure if not taken into account appropriately.

Appendix

Let X be governed by a stochastic differential equation:

$$dX = a(X,t)dt + c(X,t)dW$$

where W_t is a normalized Wiener process.

The operator $\mathscr{L}$ is defined as the differential generator of Itô process as follows [46]:

$$\begin{aligned}\mathscr{L} &= \sum_i a_i(X,t)\frac{\partial}{\partial X_i} + \frac{\partial}{\partial t} \\ &\quad + \frac{1}{2}\sum_{i,j} \text{trace}(c_i^T(X,t)c_j(X,t)\frac{\partial}{\partial X_i \partial X_j})\end{aligned}$$

References

[1] Y. Sun and B. J. Nelson, "Biological cell injection using an autonomous microrobotic system, *Int. J. of Robotics Res.*, Vol. 21, No. 10-11, pp. 861-868, 2002.

[2] H. Huang, D. Sun, J. K. Mills, and S. H. Cheng, "Robotic cell injection system with position and force control: Toward automatic batch biomanipulation, *IEEE Trans. on Robotics*, Vol. 25, No. 3, pp. 727-737, 2009.

[3] P. Kallio, T. Ritala, M. Lukkari, and S. Kuikka,"Injection guidance system for cellular microinjections, *Int. J. of Robotics Res.*, Vol. 26, No. 11-12, pp. 1303-1313, 2007.

[4] Y. Zhang, B. K. Chen, X. Liu, and Y. Sun, "Autonomous robotic pick-andplace of microobjects, *IEEE Trans. on Robotics*, Vol. 26, No. 1, pp. 200-207, 2010.

[5] M. Rakotondrabe and I. A. Ivan, "Development and force/position control of a new hybrid thermo-piezoelectric microgripper dedicated to micromanipulation tasks, *IEEE Trans. on Autom. Sci. Eng.*, Vol. 8, No. 4, pp. 824-834, 2011.

[6] EWH Jager , O. Inganas, and I. Lundstrom, "Microrobots for micrometer-size objects in aqueous media: potential tools for single-cell manipulation," *Science*, Vol. 288, No. 5475, pp. 2335-2338, 2000.

[7] E. Diller , J. Giltinan, and M. Sitti, "Independent control of multiple magnetic microrobots in three dimensions," *Int. J. of Robotics Res.*, Vol. 32, No. 5, pp. 614-631, 2013.

[8] B. J. Nelson, I. K. Kaliakatsos, and J. J. Abbott, "Microrobots for minimally invasive medicine," *Annu. Rev. Biomed. Eng.*, Vol. 12, pp. 55-85, 2010.

[9] E. B. Steager, M. S. Sakar, C. Magee, M. Kennedy, A. Cowley, and V. Kumar, "Automated biomanipulation of single cells using magnetic microrobots," *Int. J. of Robotics Res.*, Vol. 32, No. 3, pp. 346-359, 2013.

[10] T. Hayakawa, S. Fukada, and F. Arai, "Fabrication of an on-chip nanorobot integrating functional nanomaterials for single-cell punctures," *IEEE Trans. on Robotics*, Vol. 30, No. 1, pp. 59-67, 2014.

[11] Z. Zhang, Y. Huang, and C. H. Menq, "Actively controlled manipulation of a magnetic microbead using quadrupole magnetic tweezers," *IEEE Trans. on Robotics*, Vol. 26, No. 3, pp. 531-541, 2010.

[12] H. H. Cui, J. Voldman, X. F. He, and K. M. Lim, "Separation of particles by pulsed dielectrophoresis," *Lab Chip*, Vol. 9, No. 16, pp. 2306-2312, 2009.

[13] L. M. Fu, G. B. Lee, Y. H. Lin, and R. J. Yang, "Manipulation of microparticles using new modes of traveling-wave-dielectrophoretic forces: numerical Simulation and experiments," *IEEE/ASME Trans. on Mech.*, Vol. 9, No. 2, pp. 377-383, 2004.

[14] C. D. Onal, O. Ozcan, and M. Sitti, "Automated 2-D nanoparticle manipulation using atomic force microscopy," *IEEE Trans. on Nanotechnol.*, Vol. 10, No. 3, pp. 472-481, 2011.

[15] H. Xie, and S. Regnier, "High-efficiency automated nanomanipulation with parallel imaging/manipulation force microscopy," *IEEE Trans. on Nanotechnol.*, Vol. 11, No. 1, pp. 21-33, 2012.

[16] A. G. Banerjee, S. Chowdhury, W. Losert, and S. K. Gupta, "Survey on indirect optical manipulation of cells, nucleic acids, and motor proteins," *J. Biomed. Opt.*, Vol. 16, No. 5, 051302, 2011.

[17] A. Ashkin, J. M. Dziedzic, J. E. Bjorkholm, and S. Chu, "Observation of a single beam gradient force optical trap for dielectric particles," *Opt. Lett.*, Vol. 11, pp. 288-290, 1986.

[18] K. Svoboda, and S. Block, "Optical trapping of metallic rayleigh particles," *Opt. Lett.*, Vol. 19, No. 13, pp. 930C932, 1994.

[19] D. G. Grier, A Revolution in Optical Manipulation, *Nature*, Vol. 424, No. 6950, pp. 810C816, 2003.

[20] A. G. Banerjee, S. Chowdhury, and S. K. Gupta, "Optical tweezers: autonomous robots for the manipulation of biological cells," *IEEE Robotics & Automation Magazine*, Vol. 21, No. 3, pp. 81-88, 2014.

[21] S. Hu, and D. Sun, "Automatic transportation of biological cells with a robot-tweezer manipulation system," *Int. J. of Robotics Res.*, Vol. 30, No. 14, pp. 1681-1694, 2011.

[22] X. Wang, S. Chen, M. Kong, Z. Wang, K. Costa, R. A. Li, and D. Sun, "Enhanced cell sorting and manipulation with combined optical tweezer and microfluidic chip technologies," *Lab Chip*, Vol. 11, No. 21, pp. 3656-3662, 2011.

[23] F. Arai, C. Ng, H. Maruyama, A. Ichikawa, H. El-Shimy, and T. Fukuda, "On chip single-cell separation and immobilization using optical tweezers and thermosensitive hydrogel," *Lab Chip*, Vol. 5, No. 12, pp. 1399-1403, 2005.

[24] S. Hu, X. Gou, H. Han, A. Y. H. Leung, and D. Sun, "Manipulating cell adhesions with optical tweezers for study of cell-to-cell interactions, *Biomedical Nanotechnology*, Vol. 9, No. 2, pp. 281-285, 2013.

[25] X. Gou, H. Yang, T. M. Fahmy, Y. Wang, and D. Sun, "Indirect measurement of cell protrusion force utilizing a robot-aided cell manipulation system with optical tweezers for cell migration control," *Int. J. of Robotics Res.*, Vol. 33, No. 14, pp. 1782-1792, 2014.

[26] E. R. Dufresne, G. C. Spalding, M. T. Dearing, S. A. Sheets, and D. G. Grier, "Computer-generated holographic optical tweezer arrays," *Rev. Sci. Instrum.*, Vol. 72, No. 3, pp. 1810-1816, 2001.

[27] J. Leach, K. Wulff, G. Sinclair, P. Jordan, J. Courtial, L. Thomson, G. Gibson, K. Karunwi, J. Cooper, Z. J. Laczik, and M. Padgett, "Interactive approach to optical tweezers control," *Appl. Opt.*, Vol. 45, No. 5, pp. 897-903, 2005.

[28] P. J. Rodrigo, V. R. Daria, and J. Gluckstad, "Four-dimensional optical manipulation of colloidal particles," *Appl. Phys. Lett.*, 86, 074103, 2005.

[29] Y. Huang, J. Wan, M. C. Cheng, Z. Zhang, S. Jhiang, and C. H. Menq, "Three-axis rapid steering of optically propelled micro/nanoparticles," *Rev. Sci. Instrum.*, Vol. 80, No. 6, 063107, 2009.

[30] Y. Wu, D. Sun, W. Huang, and N. Xi, "Dynamics analysis and motion planning for automated cell transportation with optical tweezers," *IEEE/ASME Trans. on Mech.*, Vol. 18, No. 2, pp. 706-713, 2013.

[31] S. C. Chapin, V. Germain, and E. R. Dufresne, "Automated trapping, assembly, and sorting with holographic optical tweezers," *Optics Express*, Vol. 14, No. 26, pp. 13095-13100, 2006.

[32] A. G. Banerjee, A. Pomerance, W. Losert, and S. K. Gupta, "Developing a stochastic dynamic programming framework for optical tweezer-based

automated particle transport operations," *IEEE Trans. on Autom. Sci. Eng.*, Vol. 7, No. 2, pp. 218-227, 2010.
[33] S. Chowdhury, A. Thakur, P. Svec, C. Wang, W. Losert, and S. K. Gupta, "Automated manipulation of biological cells using gripper formations controlled by optical tweezers," *IEEE Trans. on Autom. Sci. Eng.*, Vol. 11, No. 2, pp. 338-347, 2014.
[34] X. Li, C. C. Cheah, S. Hu, and D. Sun, "Dynamic trapping and manipulation of biological cells with optical tweezers," *Automatica*, Vol. 49, No. 6, 1614-1625, 2013.
[35] C. C. Cheah, X. Li, X. Yan, and D. Sun, "Observer-based optical manipulation of biological cells with robotic tweezers," *IEEE Trans. on Robotics*, Vol. 30, No. 1, pp. 68-80, 2014.
[36] C. C. Cheah, X. Li, X. Yan, and D. Sun, "Simple PD control scheme for robotic manipulation of biological cell," *IEEE Trans. on Automatic Control*, online.
[37] Y. Tanaka, H. Kawada, K. Hirano, M. Ishikawa, and H. Kitajima, "Automated manipulation of non-spherical micro-objects using optical tweezers combined with image processing techniques," *Opt. Exp.*, Vol. 16, No. 19, pp. 15115-15122, 2008.
[38] H. Chen, and D. Sun, "Moving groups of microparticles into array with a robot-tweezers manipulation system," *IEEE Trans. on Robotics*, Vol. 28, No. 5, pp. 1069-1080, 2012.
[39] X. Yan, and D. Sun, "Multilevel-based topology design and cell patterning with robotically vontrolled optical tweezers," *IEEE Trans. on Contr. Syst. Technol.*, Vol. 23, No. 1, 176-185, 2015.
[40] A. Thakur, S. Chowdhury, P. Svec, C. Wang, W. Losert, and S. K. Gupta, "Indirect pushing based automated micromanipulation of biological cells using optical tweezers," *Int. J. of Robotics Res.*, Vol. 33, No. 8, pp. 1098-1111, 2014.
[41] R. Haghighi, and C. C. Cheah, "Optical Micromanipulation of Multiple Groups of Cells," *In Proc. IEEE Int. Conf. Robot. Autom.*, 2015 (accepted), (an extended version was submitted to *IEEE Trans. on Robotics*).
[42] S. Chowdhury, P. Svec, C. Wang, K. T. Seale, J. P. Wikswo, W. Losert, and S. K. Gupta, "Automated cell transport in optical tweezers-assisted microfluidic chambers," *IEEE Trans. on Autom. Sci. Eng.*, Vol. 10, No. 4, pp. 980-989, 2013.
[43] Y. Huang, Z. Zhang, and C. H. Menq, "Minimum-variance brownian motion control of an optically trapped probe," *Appl. Opt.*, Vol. 48, No. 3, pp. 5871-5880, 2009.
[44] A. Balijepalli, J. Gorman, S.K. Gupta, and T. LeBrun, "Significantly improved trapping lifetime of nanoparticles in an optical trap using feedback control,". *Nano Letters*, Vol. 12, No. 5, pp. 2347-2351, 2012.
[45] A. G. Banerjee, A. Balijepalli, S. K. Gupta, and T. W. LeBrun, "Generating simplified trapping probability models from simulation of optical tweezers system," *ASME J. Comput. Inf. Sci. Eng.*, Vol. 9, No. 2, 021003, 2009.
[46] H. J. Kushner, *Stochastic stability and control*. Academic Press, 1967.
[47] Q. C. Pham, N. Tabareau, and J. J. E. Slotine, "A contraction theory approach to stochastic incremental stability," *IEEE Trans. on Automatic Control*, Vol. 54, No. 4, pp. 816-820, 2009.
[48] E. Perkins, "On the Hausdorff dimension of the Brownian slow points," *Zeitschrift fr Wahrscheinlichkeitstheorie und Verwandte Gebiete*, Vol. 64, No. 3, pp. 369-399, 1983.
[49] K. Lindenberg, K. E. Shuler, J. Freeman, and T. J. Lie, "First passage time and extremum properties of Markov and independent processes," *J. Statist. Phys.*, Vol. 12, No. 3, pp. 217-251, 1975.
[50] X. Yan, C. C. Cheah, Q.-C. Pham, and J.-J. E. Slotine, "Robotic Manipulation of Micro/Nanoparticles Using Optical Tweezers with Velocity Constraints and Stochastic Perturbations," *In Proc. IEEE Int. Conf. Robot. Autom.*, pp. 797-802, 2015.
[51] M. Treiber, and A. Kesting, *Traffic Flow Dynamics Data, Models and Simulation*. Springer, 2013.
[52] W. T. Coffey, and Y. P. Kalmykov, *The Langevin Equation With Applications to Stochastic Problems in Physics, Chemistry and Electrical Engineering 3rd Edition*. World Scientific, 2012.
[53] C. Aguilar-Ibanez, M. S. Suarez-Castanon, and L. I. Rosas-Soriano, "A simple control scheme for the manipulation of a particle by means of optical tweezers," *Int. J. of Robust Nonlin.*, Vol. 21, No. 3, pp. 328-337, 2010.
[54] G. E. Uhlenbeck, and L. S. Ornstein, "On the theory of Brownian Motion," *Phys. Rev.*, Vol. 36, pp. 823-841, 1930.
[55] R. M. Simmons, J. T. Finer, S. Chu, and J. A. Spudich, "Quantitative measurements of force and displacement using an optical trap," *Biophys Journal*, Vol. 70, No. 4, pp. 1813-1822, 1996.
[56] A. Ashkin, "Forces of a single-beam gradient laser trap on a dielectric sphere in the ray optics regime," *Biophys Journal*, Vol. 61, No. 2, pp. 569-582, 1992.
[57] John J. Craig, *Adaptive control of mechanical manipulators*, Addison-Wesley, 1988.
[58] http://www.elliotscientific.com/Elliot-Scientific-E4500-Camera-Particle-Tracking-Option

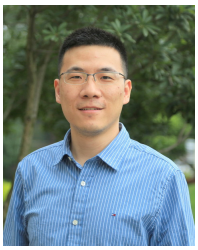

Xiao Yan received the Bachelor and PhD degrees from City University of Hong Kong in 2009 and 2013, respectively. From 2013 to 2015, he was a research fellow at the Intelligent Robotics Lab, Nanyang Technological University, Singapore. He is currently working in industry in Shenzhen, China. His research interests include multirobot control, cell manipulation, and stochastic control.

Chien Chern Cheah was born in Singapore. He received the B.E. degree in electrical engineering from National University of Singapore in 1990, and the M.E. and Ph.D. degrees in electrical engineering, both from Nanyang Technological University, Singapore, in 1993 and 1996, respectively. From 1990 to 1991, he worked as a design engineer in Chartered Electronics Industries, Singapore. He was a research fellow in the Department of Robotics, Ritsumeikan University, Japan from 1996 to 1998. He joined the School of Electrical and Electronic Engineering, Nanyang Technological University as an assistant professor in 1998. Since 2003, he has been an associate professor in Nanyang Technological University. He is an Associate Editor for Automatica.

Quang Minh Ta was born in Hanoi, Vietnam. He received the Bachelor degree in Electrical and Electronic Engineering from Hanoi University of Science and Technology, Vietnam, in 2013. He is currently working towards the Ph.D degree in the School of Electrical and Electronic Engineering, Nanyang Technological University, Singapore. His current research interests include the formation control of multi-agent systems, motion control, grasping, and robotic micromanipulation.

Pham Quang Cuong was born in Hanoi, Vietnam. He graduated from the Departments of Computer Science and Cognitive Sciences of École Normale Supérieure rue d'Ulm, Paris, France, in 2007. He obtained a PhD in Neuroscience from Université Paris VI and Collège de France in 2009. In 2010, he was a visiting researcher at the University of São Paulo, Brazil. From 2011 to 2013, he was a researcher at the University of Tokyo, supported by a fellowship from the Japan Society for the Promotion of Science (JSPS). He joined the School of Mechanical and Aerospace Engineering, NTU, Singapore, as an Assistant Professor in 2013.